ACS OMEGA

http://pubs.acs.org/journal/acsodf

Article

Crystallization, Mechanical, and Antimicrobial Properties of Diallyl Cyanuric Derivative-Grafted Polypropylene

Kun Wu, Yan Zhao, Jianqiao Li, Jinrong Yao,* Xin Chen, and Zhengzhong Shao

Cite This: *ACS Omega* 2021, 6, 12794−12800

Read Online

ACCESS | Metrics & More | Article Recommendations

ABSTRACT: A functional *N*-halamine precursor with double bonds, 1-3-diallyl-*s*-triazine-2,4,6-trione (DTT), was synthesized and grafted onto polypropylene using dicumyl peroxide (DCP) as an initiator via melt blending at 200 °C. The DTT content grafted onto the polypropylene (PP) backbone was depended on both DTT and DCP concentrations in feed. The crystallization temperature of PP increased from 116 °C (neat PP) to 123 °C (10% DTT) with the increasing DTT content. Meanwhile, the crystallization rate and relative crystallinity of PP were significantly increased after introduction of the *N*-halamine precursor. Moreover, the incorporation of DTT had partial compensation for the decreasing mechanical properties of polypropylene, which resulted from degradation. When the amount of added DTT reached up to 5%, the chlorinated DTT-modified PP sheets were able to kill 10^{5-6} cfu/mL *Escherichia coli* (CMCC 44103) and *Staphylococcus aureus* (ATCC 6538) within 10 min. The DTT-modified PP with the regenerating antibacterial property may have great potential for application in packaging, filters, and hygienic products.

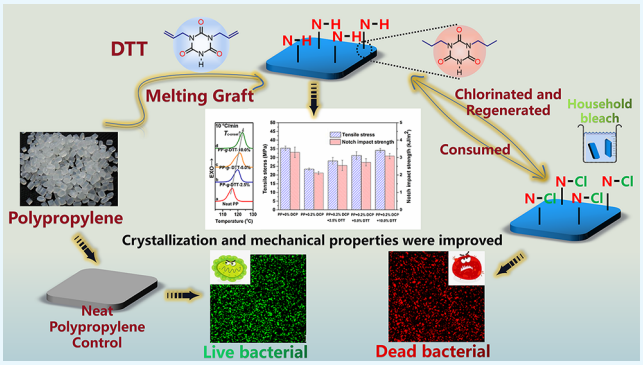

INTRODUCTION

Polypropylene (PP) is an engineering thermoplastic polymer widely employed in textiles, pipes, automobiles, and many other fields due to its several advantages, including chemical resistance, ease of processing, low price, and excellent production performance.[1−8] The research and development of high-performance and high-value-added PP plastic remains a major challenge for both academy and industry. Improvement of the crystalline properties, thermal stability, electrical conductivity, and flame-retardant properties of PP has also been introduced to increase its range of applications.[9−13] Particularly, plastics are susceptible to bacterial contamination and can act as important sources for cross-infection and cross-contamination during usage and storage. The transmission of microorganisms could be minimized by introducing antimicrobial functions. Phenol derivatives,[14−16] metal particles or ions,[17−20] quaternary ammonium,[21−23] and *N*-halamine[24−29] compounds are currently used for the preparation of numerous types of biocidal materials. *N*-halamines are a promising candidate for the preparation of antibacterial materials due to their several advantages, including their broad-spectrum antibacterial activity, nontoxicity, durability, and low environmental impact.[30,31] *N*-halamine compounds contain one or more nitrogen−halogen covalent bonds, formed by the halogenation of imide, amide, or amine groups. The antimicrobial action of *N*-halamines is believed to be a manifestation of a chemical reaction involving the transfer of positive halogens from *N*-halamine compounds to appropriate receptors in microbial cells. This process can effectively destroy or inhibit enzymatic or metabolic cell processes, resulting in the expiration of organisms.[26,27,30] In addition, their antibacterial properties are regenerated by simple exposure of the surface to household bleach, thus reactivating the *N*-halamine compounds.[31]

The incorporation of polyolefin with *N*-halamines to prepare antibacterial materials has received considerable attention. Generally, directly blending antibacterial agents into a polymer matrix seems to be a simple and common process. But leaching limits the use of the antibacterial agents and the antibacterial function cannot be restored following the loss of the antimicrobial substance, weakening their long-term use.[32] Coating or absorbing agents onto the surface of the materials is an effective method for the modification of both PP and polyethylene (PE).[33,34] However, the application of surface modification is limited because the antibacterial effect of the product is easy to disappear due to wearing. Additionally,

Received: March 1, 2021
Accepted: April 20, 2021
Published: May 3, 2021

through free-radical polymerization, immobilizing the functional *N*-halamines on polyolefin with a covalent bond during melt extrusion seems to be a facile and rapid procedure to manufacture antibacterial materials industrially. Sun and Badrossamay studied the radical graft polymerization of several cyclic and acyclic *N*-halamines onto the backbone of PP during a reactive extrusion process and obtained very effective biocidal efficacy, with a six-log reduction of Gram-positive and Gram-negative bacteria within 30−60 min of contact time.[32,35,36] However, the effects of an *N*-halamine precursor on those properties related to the industrial proceeding of polymers on the performance of materials had rarely been investigated. As is known to all that in the free-radical grafting modification reaction, the excessive initiator will lead to a large number of degradation of polypropylene, increased melt flow rate, and decreased mechanical properties, resulting in difficulties in extrusion molding and practical use.[37−39]

Herein, a novel *N*-halamine precursor with double bonds, 1-3-diallyl-*s*-triazine-2,4,6-trione (DTT), was synthesized first through the reaction of cyanuric acid with allyl bromide. DTT can easily be grafted onto the PP backbone by radical polymerization under melt blending. The grafting yield and the effects of the DTT addition on the crystallization behavior and mechanical properties of PP were assessed. The results indicated that the crystallization rate and mechanical properties of DTT-grafted PP materials were significantly increased, which are favorable to the production of PP materials. Following exposure to chlorine bleach, the DTT-modified PP sheets demonstrated highly efficient antimicrobial activities against both Gram-negative (*Escherichia coli*, CMCC 44103) and Gram-positive (*Staphylococcus aureus*, ATCC 6538) bacteria.

RESULTS AND DISCUSSION

Synthesis and Characterization of DTT. Since cyanuric acid contains three reactive imide nitrogen atoms, one is used to bind oxidative chlorine to obtain *N*-halamine, and the others can bind to the allyl groups to form reactive tethering for use in grafting onto PP. The synthesis procedure of 1-3-diallyl-*s*-triazine-2,4,6-trione (DTT) is illustrated in Scheme 1. The ^{1}H NMR spectrum of DTT (Figure 1a) exhibits four peaks (peak 1: 11.77 ppm, s, O═CN**H**C═O; peak 2: 4.28 ppm, m, NC**H$_2$**CH═CH$_2$; peak 3: 5.81 ppm, d, NCH$_2$C**H**═CH$_2$; and peak 4: 5.12 ppm, m, NCH$_2$CH═C**H$_2$**) corresponding to imide hydrogen, methylene hydrogen, and other two vinyl bond hydrogens, respectively, with a peak area ratio of 1:4:2:4. This proves that two allyl groups were successfully linked to the cyanuric acid ring. ^{13}C NMR spectrum of DTT (Figure 1b) shows five peaks at 148.89, 148.90, 43.79, 132.69, and 117.06 ppm, belonging to five different chemical surrounding carbons. These results confirm that DTT, a functional *N*-halamine precursor with double bonds, was synthesized successfully.

Scheme 1. Synthesis of 1-3-Diallyl-*s*-triazine-2,4,6-trione (DTT)

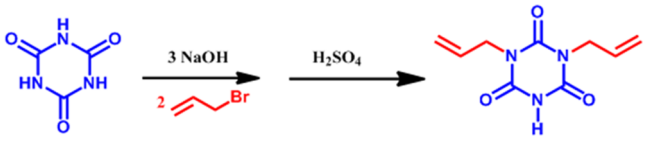

Fourier Transform Infrared Spectroscopy (FT-IR) Analysis. The DTT-grafted PP samples were named DTT-*g*-PP-*x*, where *x* is the weight percentage of the initially added DTT. Through free-radical polymerization, DTT was grafted onto the PP backbone using dicumyl peroxide (DCP) as an initiator via melt blending at 200 °C. FT-IR spectra were used to analyze the grafting polymerization of DTT (Figure 2). The

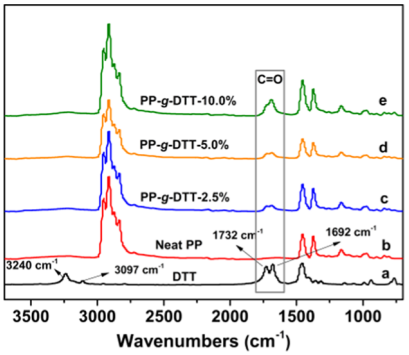

Figure 2. FT-IR spectra of DTT (a), neat PP (b), PP-*g*-DTT-2.5% (c), PP-*g*-DTT-5.0% (d), and PP-*g*-DTT-10.0% (e).

bands at 2723−2890 cm^{-1} were assigned to the C−H stretching vibrations of −CH$_2$ and −CH$_3$. Following the reaction between DTT and PP, several new peaks in the regions of 1500−1800 and 3200−3500 cm^{-1} were observed in the spectra of DTT-grafted samples. The characteristic vibrational bands that appeared at 1692 and 1735 cm^{-1} corresponded to the C═O stretching vibration of imide groups of the grafted DTT. Meanwhile, the intensities of the C═O peaks increase with the increasing DTT content. Compared with DTT, the peak at 3097 cm^{-1}, which represents the C−H stretching vibration of CH═CH$_2$, disappeared completely in all grafted samples. These findings show that the

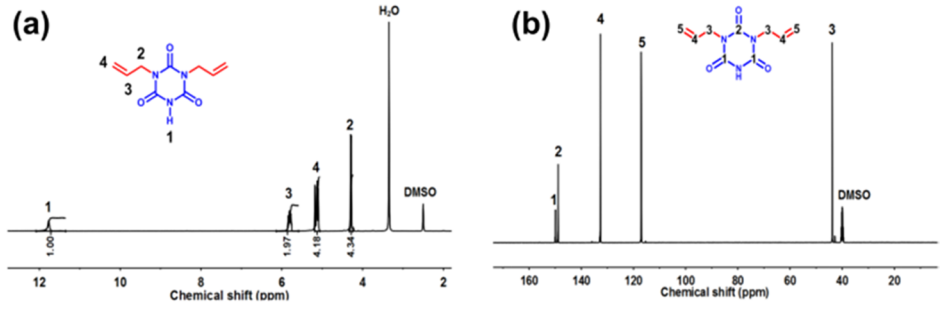

Figure 1. ^{1}H NMR (a) and ^{13}C NMR (b) spectra of 1-3-diallyl-*s*-triazine-2,4,6-trione (DTT).

https://doi.org/10.1021/acsomega.1c01100
ACS Omega 2021, 6, 12794−12800

N-halamine precursor had grafted on PP in the melting process at 200 °C.

Influence of Initiator and Monomer Contents on the Grafting Yield of DTT. The radical grafting copolymerization of PP occurred through a series of consecutive processes. First, the peroxide initiator is thermally decomposed into primary free radicals that can abstract hydrogen from the polymer backbone to generate macroradicals. The PP radicals then undergo β-scission to form secondary radicals,[37] which can still react with monomers, for example, to form grafted copolymers. The initial concentrations of the peroxide initiator and monomer affected the grafting content of DTT on PP (Figure 3). When the initial peroxide concentration was increased, the

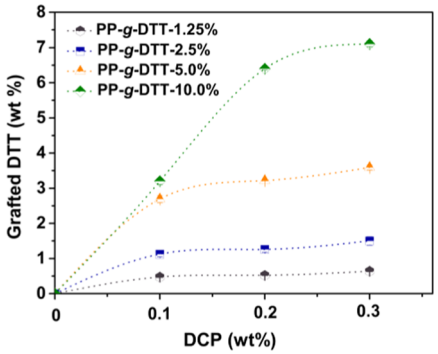

Figure 3. Influences of the DCP concentration on the grafting content of DTT at different monomer levels.

formation of more macroradicals increased the probability of polymer grafting. For the 5.0 and 10.0 wt % PP-*g*-DTT samples, the grafting yield increased with the increasing content of initial peroxide. However, at the same time, for the ratio of 1.25 and 2.5 wt % samples, the increase seems insignificant. When the initial peroxide concentration was increased from 0.1 to 0.3 wt %, the grafting contents of DTT on PP were unchanged. These phenomena may have been caused by chain transfer reactions. With the increasing peroxide concentration, chain transfer reactions are favored, resulting in homopolymerization of the monomer, which could reduce the concentration of the available monomer for the grafting reaction or side chain formation from the grafted amide N−H. Considering that the excessive initiator will cause severe degradation of the polymer, the final initiator amount applied in this study was 0.2 wt %.

Crystallization Behavior of DTT-Grafted Polypropylene. As shown in Figure 4, the X-ray diffraction (XRD) patterns of neat PP exhibit five main characteristic diffraction peaks at around 13.87, 16.62, 18.21, 20.80, and 21.52°, corresponding to the crystal planes (110), (040), (130), (111), and (131) of PP, respectively. These are the typical diffraction peaks of PP crystalline in the α form.[40] Meanwhile, similar diffraction peaks can be found in all XRD patterns of PP-*g*-DTT samples with various DTT contents, indicating that the grafting of DTT does not change the crystalline polymorphs of PP.

The crystallization behaviors of neat PP and PP-*g*-DTT samples were investigated by differential scanning calorimetry (DSC). The DSC thermograms of neat PP and PP-*g*-DTT samples are presented in Figure 5, and data are summarized in Table 1. The degree of crystallinity of PP (X_c, Table 1) was calculated according to the following equation

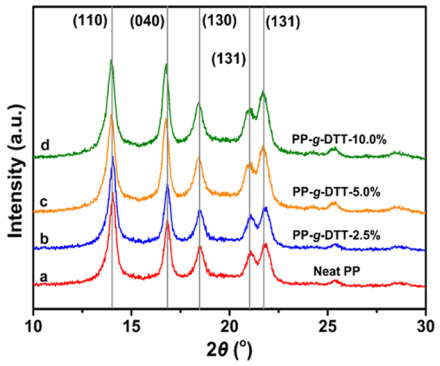

Figure 4. XRD patterns of neat PP (a), PP-*g*-DTT-2.5% (b), PP-*g*-DTT-5.0% (c), and PP-*g*-DTT-10.0% (d).

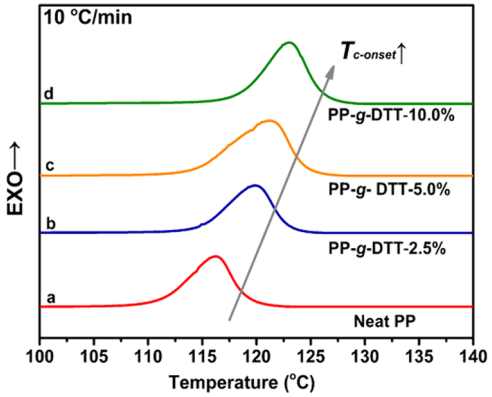

Figure 5. DSC curves of neat PP (a), PP-*g*-DTT-2.5% (b), PP-*g*-DTT-5.0% (c), and PP-*g*-DTT-10.0% (d).

Table 1. Crystallinity Properties of Neat PP, PP-*g*-DTT-2.5%, PP-*g*-DTT-5.0%, and PP-*g*-DTT-10.0%

sample	ΔH_{mc} (J/g)	T_{mc} (°C)	X_c (%)
neat PP	93.9	116.3	45.5
PP-*g*-DTT-2.5%	95.4	120.1	47.3
PP-*g*-DTT-5.0%	98.2	121.9	49.9
PP-*g*-DTT-10.0%	99.5	123.2	53.4

$$X_c = \frac{\Delta H_{mc}}{w\Delta H_s} \quad (1)$$

where ΔH_{mc} is the melting enthalpy of the sample, w is the mass percentage of PP in the sample, and ΔH_s is the complete crystallization enthalpy of PP (207 J/g).[8]

The grafting of DTT has a significant influence on PP crystallization behavior. When 2.5% of DTT was added, the melting crystallization temperature (T_{mc}) of the DTT-grafted PP sample increased from 116.3 °C (neat PP) to 120.1 °C. With the increasing DTT content, T_{mc} of PP increased to 123.2 °C (10% of DTT) gradually. The increase of T_{mc} of PP suggests that PP in the DTT-grafted samples may have a higher crystallization rate. Meanwhile, the degree of crystallinity of PP (X_c) increased as the same trend as T_{mc}.

The isothermal crystallization behavior and spherulite growth of PP were observed using polarized optical microscopy (POM) at 135 °C. As shown in Figure 6a, neat PP took nearly 40 min to complete crystallization with a nucleation induction period of 15 min. When 2.5 wt % DTT was added, the crystal morphology and size of spherulite of PP

https://doi.org/10.1021/acsomega.1c01100
ACS Omega 2021, 6, 12794−12800

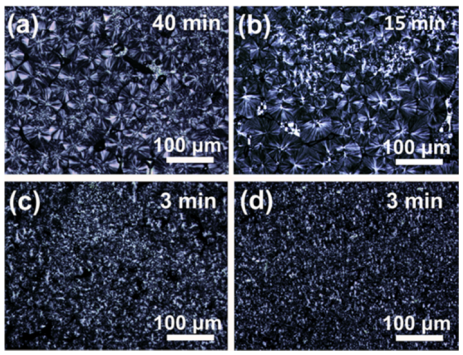

Figure 6. Polarized optical micrographs of neat PP (a), PP-*g*-DTT-2.5% (b), PP-*g*-DTT-5.0% (c), and PP-*g*-DTT-10.0% (d) isothermal crystallized at 135 °C.

in the DTT-grafted sample (Figure 6b) were similar to those of neat PP. But the time for completion of crystallization and the nucleation induction period were shortened to about 15 and 5 min, respectively. When the amount of added DTT was over 5%, the spherulite size of PP became smaller and finer obviously (Figure 6c,d), and the time to complete crystallization and nucleation induction period were less than 3 and 1 min, respectively. The analysis results of DSC and POM indicate that the grated DTT plays the role of a nucleating agent to improve the crystallization rate and crystallinity of PP.

Mechanical Properties of DTT-Grafted Polypropylene. In the mechanical property test, both neat PP and PP with 0.2% DCP only (without DTT) were used as controls. As shown in Figure 7, the tensile strength and notched impact

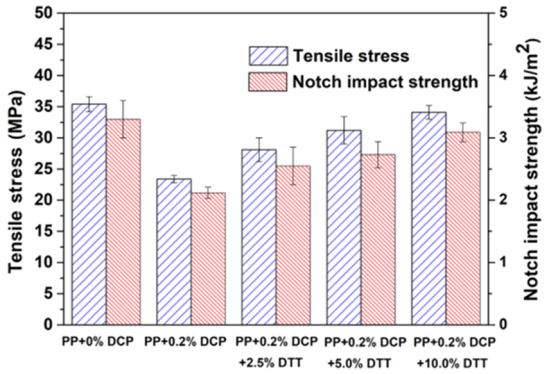

Figure 7. Tensile strength and notched impact strength of neat PP and PP-*g*-DTT samples with 0.2% DCP and various DTT concentrations.

strength of the control PP sample with DCP are 23.4 MPa and 2.12 kJ/m^2 respectively. These values are far lower than those of the pure PP sample (35.9 MPa, 3.47 kJ/m^2), and even lower than those of DTT-grated samples. When 2.5% DTT was introduced, the tensile strength and notched impact strength increased to 28.1 MPa and 2.55 kJ/m^2, respectively. As the DTT content increased to 5.0 and 10.0%, the corresponding tensile strength and notched impact strength also increased to 31.2 MPa and 34.1 MPa and 2.73 and 3.09 kJ/m^2, respectively, which gradually approached that of neat PP.

As mentioned above, the free radicals, which originated from DCP decomposition at a high temperature, can initiate the grafting polymerization and lead to the chain breaking of PP simultaneously.[37−39] The most fundamental reason for the deterioration of mechanical properties of PP samples could be due to the degradation (molecular weight reduction) of PP.[37,41] The more the DTT addition, the more obvious the effect of molecular weight compensation on the recovery of mechanical properties of DTT-grafted PP samples.

Antibacterial Efficacy. The DTT-grafted PP samples were laminated to 3 × 3 cm^2 plastic sheets with thicknesses of 1.0 mm and treated with a diluted chlorine bleach solution. The chlorinated DTT-grafted PP sheets were challenged with 10^{5-6} cfu/mL *E. coli* (Gram-negative bacteria, CMCC 44103) and *S. aureus* (Gram-positive bacteria, ATCC 6538) with a contact time of 30 min. Numerous *S. aureus* and *E. coil* cells (stained primarily green) were observed on the neat PP surface, indicating that the viable bacteria of *S. aureus* and *E. coil* were prone to the attachment on the neat PP surface and maintained their activity (Figure 8a1,b1). The chlorinated

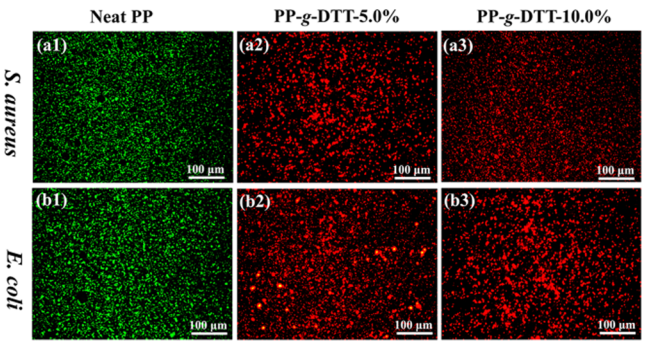

Figure 8. Fluorescence images of *S. aureus* (ATCC 6538, a1−a3) and *E. coil* (CMCC 44103, b1−b3) on surfaces of neat PP (a1, b1), PP-*g*-DTT-5.0% (a2, b2), and PP-*g*-DTT-10.0% (a3, b3) after 30 min of incubation.

PP-*g*-DTT-5.0% and PP-*g*-DTT-10.0% surfaces had a significant number of bacteria, which remained viable and displayed larger red areas (Figure 8a2,a3 and b2,b3), demonstrating that the antibacterial *N*-halamine bonded into the PP exhibited a strong capability of killing bacteria.

With the increasing DTT content, the active chlorine content on surfaces of the chlorinated DTT-grafted PP sheets increased. As shown in Table 2, the active chlorine content on surfaces of DTT-grafted PP sheets has considerable influence on the antimicrobial activity. Neat PP samples did not exhibit any detectable reduction in *E. coli* or *S. aureus* after a contact time of 60 min. The chlorinated PP-*g*-DTT-2.5% sheets, with 0.47 μg/cm^2 active chlorine, could provide 89% reduction of *E. coli* and 72% reduction of *S. aureus* after 10 min contact, respectively. As the active chlorine content on surfaces increased up to over 0.96 μg/cm^2 (PP-*g*-DTT-5%), a 100% reduction of *E. coli* and *S. aureus* could be reached within 10 min. These findings indicate that these chlorinated DTT-grafted PP materials have highly efficient antimicrobial activities against both Gram-negative and Gram-positive bacteria. Furthermore, over 75% of active chlorine could remain after the chlorinated PP-*g*-DTT-10% samples were stored in an open room environment for a month. It means that the chlorinated DTT-grafted PP materials have durable antibacterial activities to kill the adhesive microorganisms and inhibit the biofilm formation.

https://doi.org/10.1021/acsomega.1c01100
ACS Omega 2021, 6, 12794−12800

Table 2. Antibacterial Evaluation of DTT-Grafted PP Sheets against *S. aureus* (ATCC 6538) and *E. coil* (CMCC 44103) with the Contact Mode[a]

		S. aureus killed (%)			*E. coil* killed (%)		
sample	Cl^+ content ($\mu g/cm^2$)	10 min	20 min	30 min	10 min	20 min	30 min
Neat PP	0	0	0	0	0	0	0
PP-*g*-DTT-2.5%	0.47	89	96	100	72	88	100
PP-*g*-DTT-5.0%	0.96	100	100	100	100	100	100
PP-*g*-DTT-10.0%	1.94	100	100	100	100	100	100

[a]The concentration of *S. aureus* was 9.9×10^5 CFU/mL and that of *E. coil* was 7.4×10^5 CFU/mL.

CONCLUSIONS

A novel functional *N*-halamine precursor with double bonds, DTT, was synthesized and grafted onto the backbone of PP with DCP as an initiator during a reactive melt-blending process. The grafted polymerization of DTT on PP was confirmed by FT-IR analysis. With the increasing DTT content, the crystallization rate, relative crystallinity, and mechanical properties of the modified PP were increased, which are beneficial to the industrial manufacture of PP materials. After exposing in bleach solution, some of the N−H bonds of the grafted DTT could transform into N−Cl bonds, providing powerful, durable, and regenerating antimicrobial functions against both Gram-negative and Gram-positive bacteria. This *N*-halamine antibacterial polyolefin based on a novel cyanuric derivative shows potential for application in packaging, filters, and hygienic products.

EXPERIMENTAL SECTION

Materials. PP (F401, M_w = 2.2 × 10^5 g/mol, M_w/M_n = 4.85, tacticity: 96.5%) was purchased from Sinopec Yangzi Petrochemical Company (China). Cyanuric acid, allyl bromide, dicumyl peroxide (DCP), and other chemicals were purchased from Sinopharm Chemical Reagent Co., Ltd. (Shanghai, China). *E. coli* (CMCC 44103) and *S. aureus* (ATCC 6538) were provided by Shanghai Tiancheng Technology Co., Ltd. (China). Trypticase soy broth, Luria−Bertan broth, and agar were obtained from Shanghai Sangon Biotech Co., Ltd. (China). The LIVE/DEAD Baclight Bacterial Viability Kit L7012 was purchased from Molecular Probe Inc. All materials and reagents were used without further purification.

Synthesis of DTT. Cyanuric acid (5.16 g, 0.04 mol) was dissolved in 100 mL of NaOH solution (1.2 M) at room temperature. Subsequently, 9.60 g (0.08 mol) of allyl bromide was dripped slowly into the solution and stirred overnight. The reaction mixture was then neutralized (pH 6.8−7.0) with 10% H_2SO_4. Following the removal of water by rotary evaporation, washing with ethanol and deionized water several times, and drying in vacuum at 60 °C, 1-3-diallyl-*s*-triazine-2,4,6-trione (DTT) was obtained as a white powder, and its yield was 76%.

Preparation of DTT-Modified Polypropylene. A mixture of the PP granules, DTT powder, and initiator (DCP) was placed in the preheated chamber of an XSS-300 torque rheometer and melt mixed at 200 °C for 5 min at a rotation speed of 90 rpm. DTT was added at 1.25, 2.5, 5.0, and 10.0 wt %, whereas DCP was added in the range 0.1−0.3 wt %.

Determination of the Grafted Content of DTT. To remove the unreacted DTT and the homopolymer of DTT, 5 g of DTT-grafted PP samples were dissolved in 100 mL of boiling toluene. No signs of gelation were found in all samples. The hot toluene solution was then dropped into 400 mL of acetone slowly. The precipitates were collected by filtration, washed several times with acetone, and then dried at 60 °C under vacuum to reach a constant weight. The grafted percentage of DTT was calculated from the following equation[31,32,40]

$$\text{grafted percentage of (GP)\%} = (W_1 - W_2)/W_1 \times 100\% \quad (2)$$

where W_1 and W_2 are the weights of the DTT-modified PP samples before and after the dissolution/precipitation treatment, respectively. The purified samples were subsequently molded into 0.5−1 mm thick sheets at 200 °C under a pressure of 5 MPa for 5 min for further characterization and testing.

Chlorination Treatment of the DTT-Modified PP Samples. The DTT-modified PP sheets (3 × 3 cm^2) were immersed in the diluted chlorine bleach solution (containing 0.2 wt % available chlorine and 0.05 wt % Triton TX-100) for 90 min at room temperature. The plastic sheets were then washed thoroughly with excess distilled water. An iodometric titration method was used to quantify the available active chlorine content on the surfaces of the DTT-grafted PP samples.[31,32,40] The chlorine weight percentage in each sample was calculated as

$$Cl^+(\mu g)/cm^2 = \frac{35.5}{2} \times \frac{CV}{2S} \quad (3)$$

where *C* and *V* are the normality (equiv/L) and the consumed volume (L) of sodium thiosulfate, respectively, and *S* is the area (cm^2) of the plastic sheet.

Characterization. *FT-IR Spectroscopy.* Fourier transform infrared (FT-IR) spectra were recorded using a Nicolet NEXUS 470 spectrometer (Nicolet Instrument Corporation, Madison, WI) in the range of 4000−400 cm^{-1} at 64 scans per sample. The powder samples were prepared in KBr pellets, and the data collection of plastic sheet samples was completed by the attenuated total refraction (ATR) mode with an Omnic sampler.

^{1}H NMR and ^{13}C NMR. The ^{1}H NMR and ^{13}C NMR spectra were obtained using an AVANCE III 400 MHz Digital NMR spectrometer (Bruker AXS GmbH, Karlsruhe, Germany) in dimethyl sulfoxide-d6 solvent.

XRD. X-ray diffraction (XRD) patterns of PP and modified PP samples were recorded on an X'Pert PRO model (PANalytical B.V., The Netherlands) wide-angle X-ray diffractometer, using the Cu Kα radiation (λ = 1.54056 Å), within a 2θ range of 10−40° at 3°/min.

DSC. Differential scanning calorimetry (DSC) was performed using a DSC-Q2000 (TA Instruments) calorimeter in a nitrogen atmosphere. The samples were first heated to 200 °C at the rate of 20 °C/min and kept for 10 min to erase the thermal history. The samples were then cooled to 50 °C at a rate of −20 °C/min and reheated to 200 °C at a rate of 10 °C/

https://doi.org/10.1021/acsomega.1c01100
ACS Omega 2021, 6, 12794−12800

min. Melting curves were recorded at this time to obtain the melting crystallization temperature (T_{mc}) and crystallization enthalpy (ΔH_{mc}).

POM. The spherulitic growth of samples was monitored by polarized optical microscopy (POM) using an Olympus BX-51 polarized optical microscope with a hot stage (Linkam THMS 600). The samples were first heated from room temperature to 200 °C at a rate of 50 °C/min and held at 200 °C for 10 min to erase the thermal history and then cooled to 135 °C at a rate of 30 °C/min for isothermal crystallization and held at 135 °C to observe the changes in crystallization morphology of DTT-modified PP and neat PP.

Impact Strength Test. The notched Izod impact strength was tested on an XJJ-5 memorial impact tester (Changchun, China) with a hamper energy of 4.9 J, according to the Chinese Standard GB/T 1040-92 at 23 ± 0.5 °C. For each sample, the average value was derived from 5 to 7 specimens.

Tensile Strength Test. The tensile specimens were injection-molded and tested on a Sans CMT-6503 electronic material testing machine at 23 ± 0.5 °C. The preparation and test standard of the spline were carried out according to GB/T 1040-92 (the tensile rate was 50 mm/min). The maximum axial load was 10 kN. Each sample was repeated at least 5−7 times to obtain the stress−strain curve, and the average value was taken as the test result.

Antibacterial Assessment. *S. aureus* (ATCC 6538) and *E. coli* (CMCC 44103) were incubated in a static incubator at 37 °C for 24 h. The concentration of bacteria reached 10^8−10^9 colony forming units (CFU)/mL. The bacterial cells were harvested and diluted to densities of 10^5−10^6 CFU/mL with PBS solution. Both neat PP and chlorinated DTT-modified PP sheets (3 × 3 cm^2) were inoculated with 50 μL of *S. aureus* and *E. coli* bacterial suspensions in phosphate buffer solution (pH = 7) by a "sandwich test" (suspensions of the bacterial solution were added to the center of a plastic sample with an identical sample placed on top of the first one), and the actual bacterial numbers were determined by the plate counting method. After 10, 30, and 60 min of contact time, the samples were transferred to sterilized containers (5 mL of sterile 0.02 N sodium thiosulfate solution) and stirred to remove all active chlorine and rinse off surviving bacteria. Serial dilutions of the solutions contacting the surfaces were plated on trypticase agar and incubated for 24 h at 37 °C. After gradient dilution, 100 μl of each diluent was placed on the corresponding agar plate and cultured at 37 °C in a biological incubator for 24 h. Colony counts were made to determine the absence of live bacteria. The colony counts were repeated three times for each sample, and the average value was taken.

A fluorescent microscope (FM, Leica Dm4000B Germany) was used to evaluate the condition of adhered bacteria on the PP plate. Typically, the bacterial suspension (50 μL, 10^5−10^6 CFU/mL) of *S. aureus* or *E. coli* was dropped onto an aseptic PP plate surface and incubated at 37 °C for 30 min. Neat PP samples were used as controls. A freshly prepared mixture of SYTO 9 green-fluorescent and propidium iodide red-fluorescent nucleic acid stain solution (100 mL) was added following the manufacturer's instructions. After thorough mixing, the reaction was allowed to take place at room temperature in the darkness for 30 min. Absorbance values at a test wavelength of 490 nm and a reference wavelength of 660 nm were recorded.[42]

AUTHOR INFORMATION

Corresponding Author

Jinrong Yao − *State Key Laboratory of Molecular Engineering of Polymers, Department of Macromolecular Science, Laboratory of Advanced Materials, Fudan University, Shanghai 200438, China;* orcid.org/0000-0003-0868-2934; Email: yaoyaojr@fudan.edu.cn

Authors

Kun Wu − *State Key Laboratory of Molecular Engineering of Polymers, Department of Macromolecular Science, Laboratory of Advanced Materials, Fudan University, Shanghai 200438, China*

Yan Zhao − *State Key Laboratory of Molecular Engineering of Polymers, Department of Macromolecular Science, Laboratory of Advanced Materials, Fudan University, Shanghai 200438, China*

Jianqiao Li − *State Key Laboratory of Molecular Engineering of Polymers, Department of Macromolecular Science, Laboratory of Advanced Materials, Fudan University, Shanghai 200438, China*

Xin Chen − *State Key Laboratory of Molecular Engineering of Polymers, Department of Macromolecular Science, Laboratory of Advanced Materials, Fudan University, Shanghai 200438, China;* orcid.org/0000-0001-7706-4166

Zhengzhong Shao − *State Key Laboratory of Molecular Engineering of Polymers, Department of Macromolecular Science, Laboratory of Advanced Materials, Fudan University, Shanghai 200438, China;* orcid.org/0000-0001-5334-4008

Complete contact information is available at: https://pubs.acs.org/10.1021/acsomega.1c01100

Notes

The authors declare no competing financial interest.

ACKNOWLEDGMENTS

This work was supported by the National Natural Science Foundation of China (No. 51173028) and the opening projects of the State Key Laboratory for Modification of Chemical Fibers and Polymer Materials (Dong Hua University).

REFERENCES

(1) Cao, G.; Lin, H.; Kannan, P.; Wang, C.; Zhong, Y.; Huang, Y.; Guo, Z. Enhanced Antibacterial and Food Simulant Activities of Silver Nanoparticles/Polypropylene Nanocomposite Films. *Langmuir* **2018**, *34*, 14537−14545.

(2) Zhang, Y.; Fan, M.; Li, X.; Li, H.; Wang, S.; Zhu, W. Silicon-Containing Functionalized Polyolefin: Synthesis and Application. *Prog. Chem.* **2020**, *32*, 84−92.

(3) Liu, W.; Cheng, L.; Li, S. Review of electrical properties for polypropylene based nanocomposite. *Compos. Commun.* **2018**, *10*, 221−225.

(4) Yan, Y.; Hu, C.-Y.; Wang, Z.-W.; Jiang, Z.-W. Degradation of Irgafos 168 and migration of its degradation products from PP-R composite films. *Packag. Technol. Sci.* **2018**, *31*, 679−688.

(5) Sobhani, H.; Khorasani, M. M. Optimization of scratch resistance and mechanical properties in wollastonite-reinforced polypropylene copolymers. *Polym. Adv. Technol.* **2016**, *27*, 765−773.

(6) Martins, A. B.; Santana, R. M. C. Effect of carboxylic acids as compatibilizer agent on mechanical properties of thermoplastic starch and polypropylene blends. *Carbohydr. Polym.* **2016**, *135*, 79−85.

https://doi.org/10.1021/acsomega.1c01100
ACS Omega 2021, 6, 12794−12800

(7) Qiu, J.; Wang, Y.; Xing, H.; Li, M.; Liu, J.; Wang, J.; Tang, T. Preparation of Polypropylene Foams with Bimodal Cell Structure Using a Microporous Molecular Sieve as a Nucleating Agent. *Ind. Eng. Chem. Res.* **2020**, *59*, 7594−7603.
(8) Ma, G.-Q.; Sun, G.-K.; Ma, Z.; Li, J.-Q.; Sheng, J. In-line Plasma-induced Graft-copolymerization of Pentaerythritol Triacrylate onto Polypropylene. Chin. *J. Polym. Sci.* **2018**, *36*, 979−983.
(9) Cheewawuttipong, W.; Tanoue, S.; Uematsu, H.; Iemoto, Y. Thermal conductivity of polypropylene composites with hybrid fillers of boron nitride and vapor-grown carbon fiber. *Polym. Compos.* **2016**, *37*, 936−942.
(10) Andrzejewski, J.; Tutak, N.; Szostak, M. Polypropylene composites obtained from self-reinforced hybrid fiber system. *J. Appl. Polym. Sci.* **2016**, *133*, No. 43283.
(11) Bozdoğan, A.; Aksakal, B.; Koc, K.; Tsobkallo, E. S. Effect of strain level on stress relaxation and recovery behaviors of isotactic biaxially oriented polypropylene films. *J. Appl. Polym. Sci.* **2016**, *133*, No. 42948.
(12) Li, H. Y.; Li, H.; Li, Z. W.; Lin, F. C.; Wang, W. J.; Wang, B. W.; Huang, X.; Guo, X. L. Temperature dependence of self-healing characteristics of metallized polypropylene film. *Microelectron. Reliab.* **2015**, *55*, 2721−2726.
(13) Ding, L.; Xu, G.; Ge, Q.; Wu, T.; Yang, F.; Xiang, M. Effect of Fumed SiO2 on Pore Formation Mechanism and Various Performances of beta-iPP Microporous Membrane Used for Lithium-ion Battery Separator. *Chin. J. Polym. Sci.* **2018**, *36*, 536−545.
(14) Bahrami, S.; Khorasani, S. N.; Abdolmaleki, A.; Davoodi, S. M.; Farzan, A. Effect of Diphenyl carbonate derivatives and Cobalt stearate on photo-degradation of low-density polyethylene. *J. Elastomers Plast.* **2018**, *50*, 107−123.
(15) Lee, S.; Kim, N.; Cho, S.; Ryu, J.-C.; Cho, Y.; Park, J.-A.; Lee, S.-H.; Kim, J.; Choi, J.-W. Application of organic-inorganic hybrid composite particle for removal of heavy metal ions from aqueous solution and its toxicity evaluation. *Eur. Polym. J.* **2017**, *95*, 335−347.
(16) Navikaite-Snipaitiene, V.; Ivanauskas, L.; Jakstas, V.; Rueegg, N.; Rutkaite, R.; Wolfram, E.; Yildirim, S. Development of antioxidant food packaging materials containing eugenol for extending display life of fresh beef. *Meat Sci.* **2018**, *145*, 9−15.
(17) Ahmad, N.; Sultana, S.; Faisal, S. M.; Ahmed, A.; Sabir, S.; Khan, M. Z. Zinc oxide-decorated polypyrrole/chitosan bionanocomposites with enhanced photocatalytic, antibacterial and anticancer performance. *RSC Adv.* **2019**, *9*, 41135−41150.
(18) Siddiqui, N.; Al Masum, A.; Uddin, M. R.; Mandal, S.; Sengupta, M.; Islam, M. M.; Mukhopadhyay, S. Elucidating the chemical and biochemical applications of Citrus sinensis-mediated silver nanocrystal. *J. Biomol. Struct. Dyn.* **2019**, *37*, 4863−4874.
(19) Mehra, C.; Gala, R.; Kakatkar, A.; Kumar, V.; Khurana, R.; Chatterjee, S.; Kumar, N. N.; Barooah, N.; Bhasikuttan, A. C.; Mohanty, J. Cooperative enhancement of antibacterial activity of sanguinarine drug through p-sulfonatocalix 6 arene functionalized silver nanoparticles. *Chem. Commun.* **2019**, *55*, 14275−14278.
(20) Precious Ayanwale, A.; Yobanny Reyes-Lopez, S. ZrO2-ZnO Nanoparticles as Antibacterial Agents. *ACS Omega* **2019**, *4*, 19216−19224.
(21) Oh, J.; Kim, S.-J.; Oh, M.-K.; Khan, A. Antibacterial properties of main-chain cationic polymers prepared through amine-epoxy 'Click' polymerization. *RSC Adv.* **2020**, *10*, 26752−26755.
(22) Li, W.; Ouyang, H.; Chen, L.; Yuan, D.; Zhang, Y.; Yao, Y. A comparative study on dinuclear and mononuclear aluminum methyl complexes bearing piperidyl-phenolato ligands in ROP of epoxides. *Inorg. Chem.* **2016**, *55*, 6520−6524.
(23) Zeng, W.; He, J.; Liu, F. Preparation and properties of antibacterial ABS plastics based on polymeric quaternary phosphonium salts antibacterial agents. *Polym. Adv. Technol.* **2019**, *30*, 2515−2522.
(24) Sun, G.; Worley, S. D. Chemistry of durable and regenerable biocidal textiles. *J. Chem. Educ.* **2005**, *82*, 60−64.
(25) Kenawy, E. R.; Worley, S. D.; Broughton, R. The chemistry and applications of antimicrobial polymers: A state-of-the-art review. *Biomacromolecules* **2007**, *8*, 1359−1384.
(26) Sun, Y. Y.; Sun, G. Durable and refreshable polymeric *N*-halamine biocides containing 3-(4′-vinylbenzyl)-5,5-dimethylhydantoin. *J. Polym. Sci., Part A: Polym. Chem.* **2001**, *39*, 3348−3355.
(27) Zhao, Y.; Wei, B.; Wu, M.; Zhang, H.; Yao, J.; Chen, X.; Shao, Z. Preparation and characterization of antibacterial poly(lactic acid) nanocomposites with *N*-halamine modified silica. *Int. J. Biol. Macromol.* **2020**, *155*, 1468−1477.
(28) Kocer, H. B.; Cerkez, I.; Worley, S. D.; Broughton, R. M.; Huang, T. S. Polymeric Antimicrobial *N*-halamine Epoxides. *ACS Appl. Mater. Interfaces* **2011**, *3*, 2845−2850.
(29) Liu, C.; Dai, Z. J.; Zhou, R.; Ke, Q. F.; Huang, C. Fabrication of Polypropylene-g-(Diallylamino Triazine) Bifunctional Nonwovens with Antibacterial and Air Filtration Activities by Reactive Extrusion and Melt-Blown Technology. *J. Chem.* **2019**, *2019*, No. 3435095.
(30) Ren, X. H.; Zhu, C. Y.; Kou, L.; Worley, S. D.; Kocer, H. B.; Broughton, R. M.; Huang, T. S. Acyclic *N*-halamine Polymeric Biocidal Films. *J. Bioact. Compat. Polym.* **2010**, *25*, 392−405.
(31) Yao, J. R.; Sun, Y. Y. Preparation and characterization of polymerizable hindered amine-based antimicrobial fibrous materials. *Ind. Eng. Chem. Res.* **2008**, *47*, 5819−5824.
(32) Badrossamay, M. R.; Sun, G. Preparation of rechargeable biocidal polypropylene by reactive extrusion with diallylamino triazine. *Eur. Polym. J.* **2008**, *44*, 733−742.
(33) Zhao, N.; Liu, S. Thermoplastic semi-IPN of polypropylene (PP) and polymeric *N*-halamine for efficient and durable antibacterial activity. *Eur. Polym. J.* **2011**, *47*, 1654−1663.
(34) Cerkez, I.; Worley, S. D.; Broughton, R. M.; Huang, T. S. Antimicrobial surface coatings for polypropylene nonwoven fabrics. *React. Funct. Polym.* **2013**, *73*, 1412−1419.
(35) Badrossamay, M. R.; Sun, G. Graft Polymerization of N-tert-Butylacrylamide Onto Polypropylene During Melt Extrusion and Biocidal Properties of its Products. *Polym. Eng. Sci.* **2009**, *49*, 359−368.
(36) Badrossamay, M. R.; Sun, G. Acyclic halamine polypropylene polymer: Effect of monomer structure on grafting efficiency, stability and biocidal activities. *React. Funct. Polym.* **2008**, *68*, 1636−1645.
(37) Azizi, H.; Ghasemi, I. Investigation on influence of peroxidedegradation process on rheological properties of polypropylene. *Iran. Polym. J.* **2005**, *14*, 465−471.
(38) Mandal, D. K.; Bhunia, H.; Bajpai, P. K.; Dubey, K. A.; Varshney, L.; Madhu, G. Thermo-oxidative degradation kinetics of grafted polypropylene films. *Radiat. Eff. Defects Solids* **2017**, *172*, 878−895.
(39) Nesvadba, P. Radicals and Polymers. *Chimia* **2018**, *72*, 456−476.
(40) An, Y.; Wang, S.; Li, R.; Shi, D.; Gao, Y.; Song, L. Effect of different nucleating agent on crystallization kinetics and morphology of polypropylene. *e-Polymers* **2019**, *19*, 32−39.
(41) Coiai, S.; Passaglia, E.; Aglietto, M.; Ciardelli, F. Control of degradation reactions during radical functionalization of polypropylene in the melt. *Macromolecules* **2004**, *37*, 8414−8423.
(42) Wu, K.; Li, J.; Chen, X.; Yao, J.; Shao, Z. Synthesis of novel multi-hydroxyl *N*-halamine precursors based on barbituric acid and their applications in antibacterial poly(ethylene terephthalate) (PET) materials. *J. Mater. Chem. B* **2020**, *8*, 8695−8701.

https://doi.org/10.1021/acsomega.1c01100
ACS Omega 2021, 6, 12794−12800